Available online at www.sciencedirect.com

ScienceDirect

IFAC-PapersOnLine 49-8 (2016) 130–135

State Feedback Stabilization of the Linearized Bilayer *Saint-Venant* Model

Ababacar Diagne [*] **Shuxia Tang** [**] **Mamadou Diagne** [***] **Miroslav Krstic** [**]

[*] *Division of Scientific Computing, Department of Information Technology, Uppsala University, Box 337, 75105 Uppsala, Sweden (email: ababacar.diagne@it.uu.se).*
[**] *Department of Mechanical & Aerospace Engineering, University of California, San Diego, La Jolla, CA 92093-0411, USA (e-mail: sht015@ucsd.edu; krstic@ucsd.edu)*
[***] *Department of Mechanical Engineering, University of Michigan G.G. Brown Laboratory 2350 Hayward Ann Arbor MI 48109, USA (e-mail: mdiagne@umich.edu)*

Abstract We consider the problem of stabilizing the bilayer *Saint-Venant* model, which is a coupled system of two rightward and two leftward convecting transport partial differential equations (PDEs). In the stability proofs, we employ a Lyapunov function in which the parameters need to be successively determined. To the best of the authors' knowledge, this is the first time this kind of Lyapunov function is employed, and this result is the first one on the stabilization of the linearized bilayer *Saint-Venant* model. Numerical simulations of the bilayer *Saint-Venant* problem are also provided to verify the result.

Keywords: Backstepping control; Bilayer *Saint-Venant* model; State feedback stabilization; State-varying coefficients; coupled PDEs.

1. INTRODUCTION

In this paper, the 1D two-layer Saint-Venant model that consists of the superposition of two immiscible fluids with different constant densities is presented. The derivation of the bilayer model can be found in Audusse et al. (2011) and Bouchut and Morales (2008). One can also find some results on mathematical analysis of the related problem in Narbona-Reina and Zabsonre (2009) and Munoz-Ruiz et al. (2003). The two-layer model is often used to describe transcritical regime of shallow-water flow and sediment dynamics Majd and Sanders (2014); Savary et al. (2006) which may occur when a transition from subcritical to supercritical low regime is incorporated into the well known Saint-Venant Exner model Diagne et al. (2016). An analysis of the dynamics of the two-layers model is proposed in Kim and LeVeque (2008) for the analysis of tsunamis generated by an underwater landslide.

PDE backstepping control approach has been successfully employed for the feedback stabilization of various classes of PDEs Di Meglio et al. (2013); Krstic and Smyshlyaev (2008). In the present work, a general system, which consists of m rightward and n leftward transport PDEs with spatially varying coefficients, is exponentially stabilized by m boundary input backstepping controllers. Our backstepping controller design idea can be referred to Hu et al. (2015), in which the stabilization problem for the general coupled heterodirectional system of hyperbolic types with an arbitrary number of equations convecting in both directions is definitely solved. In our stability proofs, we employ a Lyapunov function in which the parameters need to be successively determined. Then, applying this general stabilization result to the 1D bilayer *Saint-Venant* problem with ($n = m = 2$), we achieve exponential stabilization with two boundary input controllers.

2. PROBLEM STATEMENT

2.1 The 1D nonlinear bilayer Saint-Venant model

The 1D two-layer *Saint-Venant* model is governed by the following equations

$$\frac{\partial H_1}{\partial t} + \frac{\partial (H_1 U_1)}{\partial x} = 0, \tag{1a}$$

$$\frac{\partial U_1}{\partial t} + U_1 \frac{\partial U_1}{\partial x} + g\frac{\partial H_1}{\partial x} + g\frac{\partial H_2}{\partial x} + g\frac{\partial B}{\partial x} = S_1^f, \tag{1b}$$

$$\frac{\partial H_2}{\partial t} + \frac{\partial (H_2 U_2)}{\partial x} = 0, \tag{1c}$$

$$\frac{\partial U_2}{\partial t} + U_2 \frac{\partial U_2}{\partial x} + g\frac{\partial H_2}{\partial x} + g\frac{\rho_1}{\rho_2}\frac{\partial H_1}{\partial x} + g\frac{\partial B}{\partial x} = S_2^f. \tag{1d}$$

In (1), the index 1 refers to the upper layer and the index 2 to the lower one, as depicted in Figure 2.1. The unknown state variables H_i, U_i and B represent the thickness of the i-th layer, the velocity and the height of the sediment layer, respectively. Each layer is assumed to have a constant density ρ_i, $i = 1, 2$ ($\rho_1 < \rho_2$). The system contains the source terms due to the bottom topography and the friction term. The quantities S_1^f and S_2^f stand as the friction between the two layers, and they are given by

10.1016/j.ifacol.2016.07.431

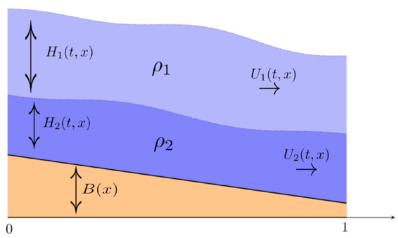

Figure 1. Bilayer shallow water flows.

$$S_1^f = -C_f|U_1 - U_2|(U_1 - U_2) \tag{2}$$

and

$$S_2^f = rC_f|U_1 - U_2|(U_1 - U_2). \tag{3}$$

Define a vector $W = [H_1,\ U_1,\ H_2,\ U_2]^T$, a ratio $r = \dfrac{\rho_1}{\rho_2}$ and a map

$$F(W) = \begin{bmatrix} H_1U_1 \\ \dfrac{U_1^2}{2} + g(H_1 + H_2) \\ H_2U_2 \\ \dfrac{U_2^2}{2} + g(H_2 + rH_1) \end{bmatrix} \tag{4}$$

then we could recast equation (1) under the form of

$$\frac{\partial W}{\partial t} + \frac{\partial F(W)}{\partial x} = S(x, W), \tag{5}$$

where

$$S(x,W) = \left(0 \quad S_1^f - g\frac{\partial B}{\partial x} \quad 0 \quad S_2^f - g\frac{\partial B}{\partial x}\right)^T. \tag{6}$$

By considering the Jacobian matrix A from (5), we could rewrite the equation (5) into a quasi-linear form as

$$\boldsymbol{\frac{\partial W}{\partial t} + A(W)\frac{\partial W}{\partial x} = S(x, W)}, \tag{7}$$

where

$$A(W) = \begin{bmatrix} U_1 & H_1 & 0 & 0 \\ g & U_1 & g & 0 \\ 0 & 0 & U_2 & H_2 \\ rg & 0 & g & U_2 \end{bmatrix} \tag{8}$$

Simple and exact analytical expression of the four eigenvalues of A is not obvious. Complicate expression can be obtained tediously by applying the Cardano-Vieta method. For the case of $r \approx 1$ and $U_1 \approx U_2$, a first order approximation of the eigenvalues is given in Nieto et al. (July 2011); Abgrall and Karni (2009).

In this work, we consider the case where $r \ll 1$, namely, when the bottom fluid is much thicker than the upper fluid. Moreover, recall that our problem is to consider the boundary controller design to stabilize (7).

2.2 Linearization of the Saint-Venant model

We denote the steady-state associated to the system (7) by $W^* = (H_1^*, U_1^*, H_2^*, U_2^*)$, which satisfies the following equation of a compact form:

$$\boldsymbol{A(W^*)\partial_x W^* = S(x, W^*)}. \tag{9}$$

To obtain a constant steady-state, we work in the sequel with a flat bathymetry ($\partial_x B = 0$). A constant steady-state of the two-layer Saint-Venant equations can be characterized by:

$$\begin{cases} H_1^*U_1^* = \text{constant}, \qquad H_2^*U_2^* = \text{constant}, \\ \dfrac{U_1^{*2}}{2} + g(H_1^* + H_2^*) = -C_f|U_1^* - U_2^*|(U_1^* - U_2^*), \\ \dfrac{U_2^{*2}}{2} + g(H_2^* + rH_1^*) = rC_f|U_1^* - U_2^*|(U_1^* - U_2^*). \end{cases} \tag{10}$$

In order to linearize the governing equations around the steady state, we define the deviation (h_1, u_1, h_2, u_2) of the state (H_1, U_1, H_2, U_2) with respect to the steady-state $(H_1^*, U_1^*, H_2^*, U_2^*)$ by:

$$\begin{cases} h_1 = H_1 - H_1^*, \qquad u_1 = U_1 - U_1^*, \\ h_2 = H_2 - H_2^*, \qquad u_2 = U_2 - U_2^*. \end{cases} \tag{11}$$

Then, the linearized version of (7) can be written in a matrix form as

$$\partial_\mathbf{t}\mathbf{U} + \mathbf{A}^*\partial_\mathbf{x}\mathbf{U} = \mathbf{S_l}(\mathbf{U}), \tag{12}$$

where

$$U = (h_1, u_1, h_2, u_2)^T, \qquad A^* = A(W^*),$$

and

$$S_l(U) = [0 \ \ -\alpha_s^f(u_1 - u_2) \ 0 \ r\alpha_s^f(u_1 - u_2)]^T$$

with

$$\alpha_s^f = 2C_f|U_1^* - U_2^*|.$$

We consider a constant steady state here for the sake of readability and simplicity in the presentation of the linear model.

2.3 Linearized Saint-Venant model in Riemann coordinates

We are to explore the system eigenstructure of the linear form (12) in this subsection. The characteristic equation derived from the matrix A^* is

$$\Theta = rg^2H_1^*H_2^*, \tag{13}$$

where

$$\Theta = \Big((\lambda - U_1^*)^2 - gH_1^*\Big)\Big((\lambda - U_2^*)^2 - gH_2^*\Big). \tag{14}$$

For the case $r = 0$, straightforward calculations lead to the following real eigenvalues for A^*:

$$\begin{matrix} \lambda_1 = U_1^* - \sqrt{gH_1^*}, & \lambda_2 = U_1^* + \sqrt{gH_1^*}, \\ \lambda_3 = U_2^* - \sqrt{gH_2^*}, & \lambda_4 = U_2^* + \sqrt{gH_2^*}. \end{matrix} \tag{15}$$

We notice that the eigenvalues in this case are those corresponding to each layer separately. Following the results in Schijf and Schonfeld (Sept. (1953), the eigenvalues for the system (7) in the case of $r \ll 1$ i.e $\rho_1 \ll \rho_2$ approach to those given in (15). From (15), the internal and external characteristics travel at different speeds, and indeed, the lower layer characteristics moves much slower than the upper ones in the case of $r \ll 1$. Let us now recast the equation (12) into a diagonal form. For a given eigenvalue λ_k $(k = 1, 2, 3, 4)$ of the matrix A^*, the associated right eigenvector is expressed by

$$V_k = \begin{bmatrix} 1 \\ \dfrac{\lambda_k - U_1^*}{H_1^*} \\ \dfrac{(\lambda_k - U_1^*)^2 - gH_1^*}{gH_1^*} \\ \dfrac{(\lambda_k - U_2^*)((\lambda_k - U_1^*)^2 - gH_1^*)}{gH_1^*H_2^*} \end{bmatrix} \tag{16}$$

Some computations lead to the associated left eigenvector $L_k,\ k \in \{1,2,3,4\}$:

$$L_k = -\left(\prod_{i\in\{1,2,3,4\}/\{k\}}\right)^{-1}\begin{bmatrix} l_{k,1} & l_{k,2} & l_{k,3} & l_{k,4}\end{bmatrix}^{\mathrm{T}}, \tag{17}$$

where

$$l_{k,1} = U_1^{*3} - (\mathrm{tr}(A^*) - \lambda_k)(U_1^{*2} + gH_1^*) + f_k + 3gH_1^* - \frac{\det(A^*)}{\lambda_k}, \tag{18}$$

$$l_{k,2} = 3H_1^*U_1^{*2} - 2H_1^*U_1^*(\mathrm{tr}(A^*) - \lambda_k) + H_1^*(f_k + gH_1^*), \tag{19}$$

$$l_{k,3} = gH_1^*(7U_1^* - \lambda_k), \quad l_{k,4} = gH_1^*H_2^*. \tag{20}$$

Here and in the sequel, T, tr and det denote the transpose, trace and determinant, respectively. The quantities f_k are defined by:

$$f_1 = (\lambda_3 + \lambda_2)\lambda_4 + \lambda_2\lambda_3,\ f_2 = (\lambda_3 + \lambda_1)\lambda_4 + \lambda_1\lambda_3, \tag{21}$$

$$f_3 = (\lambda_2 + \lambda_1)\lambda_4 + \lambda_1\lambda_2,\ f_4 = (\lambda_1 + \lambda_2)\lambda_3 + \lambda_1\lambda_2. \tag{22}$$

We are to express the linear version (12) of the governing equations in term of the characteristic coordinates or Riemann Invariants. Multiplying the equation (12) by the left eigenvectors L_k (each for a given eigenvalue λ_k) of the matrix A^*, we get that the characteristic coordinates (Riemann Invariants) ξ_k are:

$$\xi_k = L_k^T U = -\left(\prod_{i\in\{1,2,3,4\}/\{k\}}\right)^{-1} \times \left[l_{k,1}h_1 + l_{k,2}u_1 + l_{k,3}h_2 + l_{k,4}u_2\right]. \tag{23}$$

Therefore, we can express the variables h_1, u_1, h_2 and u_2 in term of the Riemann Invariants:

$$\begin{cases} h_1 = \xi_1 + \xi_2 + \xi_3 + \xi_4, \\ u_1 = \gamma_1\xi_1 + \gamma_2\xi_2 + \gamma_3\xi_3 + \gamma_4\xi_4, \\ h_2 = \beta_1\xi_1 + \beta_2\xi_2 + \beta_3\xi_3 + \beta_4\xi_4, \\ u_2 = \alpha_1\xi_1 + \alpha_2\xi_2 + \alpha_3\xi_3 + \alpha_4\xi_4, \end{cases} \tag{24}$$

where

$$\gamma_k = \frac{\lambda_k - 1}{H_1^*}, \tag{25}$$

$$\beta_k = \frac{1}{gH_1^*}\Big(U_1^{*2} + 2(\lambda_k - 1)U_1^* - \lambda_k^2 + gH_1^*\Big), \tag{26}$$

and

$$\alpha_k = \frac{1}{gH_1^*H_2^*}\big((gH_1^*\beta_k - 2\lambda_k^2)U_2^* + 3U_1^{*3} + 7(\lambda_k - 1)U_1^{*2} + 2(gH_1^* - 2\lambda_k^2)U_1^* + \lambda_k^2(\mathrm{tr}(A^*) - \lambda_k) + gH_1^*(\lambda_k + 2)\big). \tag{27}$$

We introduce the following more compact notations:

$$\boldsymbol{\xi} = (\xi_1\ \xi_2\ \xi_3\ \xi_4)^T, \tag{28}$$

and

$$\boldsymbol{\Lambda} = \mathrm{diag}\{\lambda_1, \lambda_2, \lambda_3, \lambda_4\}. \tag{29}$$

Using the characteristic coordinates, we recast the equation (12) into the following form:

$$\boldsymbol{\partial_t\xi + \Lambda\partial_x\xi = M\xi,} \tag{30}$$

where

$$M(W^*) = \big(0,\ \alpha_s^f,\ 0,\ -r\alpha_s^f\big)^T \times (\alpha_1 - \gamma_1,\ \alpha_2 - \gamma_2,\ \alpha_3 - \gamma_3,\ \alpha_4 - \gamma_4). \tag{31}$$

We consider the case where both layers have a subcritical flow regime. Define the state vectors

$$u(t,x) = (\xi_2, \xi_4)^{\mathrm{T}},\ v(t,x) = (\xi_1, \xi_3)^{\mathrm{T}},$$

and introduce the transport speed matrices

$$\boldsymbol{\Lambda}^{\mathrm{r}} = \mathrm{diag}\{\lambda_2, \lambda_4\},\ -\boldsymbol{\Lambda}^{\mathrm{l}} = \mathrm{diag}\{\lambda_1, \lambda_3\}.$$

Then, the system (30) can be rewritten as

$$\partial_t u(t,x) + \Lambda^{\mathrm{r}}\partial_x u(t,x) = S^{\mathrm{r}}u(t,x) + S^{\mathrm{l}}v(t,x), \tag{32}$$

$$\partial_t v(t,x) - \Lambda^{\mathrm{l}}\partial_x v(t,x) = 0, \tag{33}$$

where

$$S^{\mathrm{r}} = \begin{bmatrix} \alpha_s^f(\alpha_1 - \gamma_1) & \alpha_s^f(\alpha_2 - \gamma_2) \\ r\alpha_s^f(\gamma_1 - \alpha_1) & r\alpha_s^f(\gamma_2 - \alpha_2)\end{bmatrix}, \tag{34}$$

$$S^{\mathrm{l}} = \begin{bmatrix} \alpha_s^f(\alpha_3 - \gamma_3) & \alpha_s^f(\alpha_4 - \gamma_4) \\ r\alpha_s^f(\gamma_3 - \alpha_3) & r\alpha_s^f(\gamma_4 - \alpha_4)\end{bmatrix}. \tag{35}$$

To close the writing of the system (32)-(33), we enclose to it the following boundary and initial conditions:

$$u(t,0) = Q_0v(t,0) \text{ and } v(t,1) = R_1u(t,1) + \mathfrak{U}(t), \tag{36}$$

$$u(0,x) = u_0(x) \text{ and } v(0,x) = v_0(x), \tag{37}$$

where Q_0, $R_1 \in \mathcal{M}_{2,2}(\mathbb{R})$, and $\mathfrak{U}(t)$ consists of the boundary controllers we need to design.

3. CONTROLLER DESIGN OF A GENERAL SYSTEM

In this section, we consider the backstepping controller design of a more general system, which could includes the *Saint-Venant* model as a special case. While solving our problem with the *Saint-Venant* model, it is also worth noting that the result derived in this section could be treated as a full theoretical result by itself.

3.1 A more general control system

The more general system discussed in this section is

$$\partial_t u(t,x) + \Lambda^{\mathrm{r}}(x)\partial_x u(t,x) = S^{\mathrm{r}}(x)u(t,x) + S^{\mathrm{l}}(x)v(t,x) \tag{38}$$

$$\partial_t v(t,x) - \Lambda^{\mathrm{l}}(x)\partial_x v(t,x) = S^{\mathrm{o}}(x)u(t,x), \tag{39}$$

where

$$u(x,t) = [u_1(x,t),\ u_2(x,t),\ \ldots,\ u_n(x,t)], \tag{40}$$

$$v(x,t) = [v_1(x,t),\ v_2(x,t),\ \ldots,\ v_m(x,t)] \tag{41}$$

are the systems states. The matrices

$$\boldsymbol{\Lambda}^{\mathbf{r}}(x) = \mathrm{diag}\left[\lambda_1^{\mathrm{r}}(x),\ \lambda_2^{\mathrm{r}}(x),\ \cdots,\ \lambda_n^{\mathrm{r}}(x)\right], \tag{42}$$

$$\boldsymbol{\Lambda}^{\mathbf{l}}(x) = \mathrm{diag}\left[\lambda_1^{\mathrm{l}}(x),\ \lambda_2^{\mathrm{l}}(x),\ \cdots,\ \lambda_m^{\mathrm{l}}(x)\right], \tag{43}$$

subject to the restriction

$$0 < \lambda_1^{\mathrm{r}}(x) < \lambda_2^{\mathrm{r}}(x) < \cdots < \lambda_n^{\mathrm{r}}(x), \tag{44}$$

$$0 < \lambda_m^{\mathrm{l}}(x) < \lambda_2^{\mathrm{l}}(x) < \cdots < \lambda_1^{\mathrm{l}}(x), \tag{45}$$

and the in-domain parameters are given as

$$S^{\mathrm{r}}(x) = \{S_{ij}^{\mathrm{r}}(x)\}_{1\le i\le n, 1\le j\le n}, \tag{46}$$

$$S^{\mathrm{l}}(x) = \{S_{ij}^{\mathrm{l}}(x)\}_{1\le i\le n, 1\le j\le m}, \tag{47}$$

$$S^{\mathrm{o}}(x) = \{S_{ij}^{\mathrm{o}}(x)\}_{1\le i\le n, 1\le j\le m}. \tag{48}$$

The system is also equipped with the following boundary and initial conditions:

$$u(t,0) = Q_0v(t,0) \text{ and } v(t,1) = R_1u(t,1) + \mathfrak{U}(t), \tag{49}$$

$$u(0,x) = u_0(x) \text{ and } v(0,x) = v_0(x), \tag{50}$$

where the boundary parameters Q_0, $R_1 \in \mathcal{M}_{m,n}(\mathbb{R})$ are given as

$$R_1 = \{r_{ij}\}_{1\le i\le m, 1\le j\le n}. \tag{51}$$

$$Q_0 = \{q_{ij}(x)\}_{1\le i\le n, 1\le j\le m}, \tag{52}$$

and $\mathfrak{U}(t)$ denotes the boundary controllers.

3.2 Target system

First, we construct a backstepping transformation to map the system (38)-(39) into a target system with desirable stability property, which follows from the one constructed in Hu et al. (2015). Consider the following target system

$$\partial_t \epsilon(t,x) + \Lambda^{\mathrm{r}}(x)\partial_x \epsilon(t,x) = S^{\mathrm{r}}(x)\epsilon(t,x) + S^{\mathrm{l}}(x)\beta(t,x) + \int_0^x C^{\mathrm{r}}(x,\xi)\epsilon(\xi)d\xi + \int_0^x C^{\mathrm{l}}(x,\xi)\beta(\xi)d\xi \quad (53)$$

$$\partial_t \beta(t,x) - \Lambda^{\mathrm{l}}(x)\partial_x \beta(t,x) = \Delta(x)\beta(0,t) \quad (54)$$

with the following boundary conditions

$$\epsilon(t,0) = Q_0\beta(t,0) \text{ and } \beta(t,1) = 0, \quad (55)$$

where

$$\Delta(x) = \begin{bmatrix} 0 & \cdots & \cdots & 0 \\ \delta_{2,1}(x) & \ddots & \ddots & \vdots \\ \vdots & \ddots & \ddots & \vdots \\ \delta_{m,1}(x) & \cdots & \delta_{m,m-1}(x) & 0 \end{bmatrix}, \quad (56)$$

and C^{r}, C^{l} are matrices of functions defined on the triangular domain

$$\mathbb{T} = \Big\{(x,\xi) \in \mathbb{R}^2 | \; 0 \le \xi \le x \le 1\Big\}.$$

Here, $\Delta(x)$, C^{r}, C^{l} are all to be determined by introducing a backstepping transformation later.

3.3 Backstepping controller design

In order to map the system (38)-(39) into the desired target system (53)-(55), we consider the following backstepping transformation

$$\begin{pmatrix} \epsilon(t,x) \\ \beta(t,x) \end{pmatrix} = \begin{pmatrix} u(t,x) \\ v(t,x) \end{pmatrix} - \int_0^x \begin{pmatrix} 0 & 0 \\ G_{21}(x,\xi) & G_{22}(x,\xi) \end{pmatrix} \begin{pmatrix} u(t,\xi) \\ v(t,\xi) \end{pmatrix} d\xi. \quad (57)$$

Here, the to-be-determined kernel functions G_{21} and G_{22} are defined on the domain $\mathbb{T}$. From the system equations (38)–(50) and (53)–(55) and through some calculations and integration by parts, it follows that G_{21} and G_{22} need to satisfy the following system of equations:

$$\partial_\xi G_{21}(x,\xi)\mathbf{\Lambda}^{\mathbf{r}}(\xi) - \mathbf{\Lambda}^{\mathbf{l}}(x)\partial_x G_{21}(x,\xi) = -G_{21}(x,\xi)\frac{d\mathbf{\Lambda}^{\mathbf{r}}(\xi)}{d\xi} - G_{21}(x,\xi)S^{\mathrm{r}}(\xi) - G_{22}(x,\xi)S^{\mathrm{o}}(\xi) \quad (58)$$

$$\partial_\xi G_{22}(x,\xi)\mathbf{\Lambda}^{\mathbf{r}}(\xi) + \mathbf{\Lambda}^{\mathbf{l}}(x)\partial_x G_{22}(x,\xi) = -G_{22}(x,\xi)\frac{d\mathbf{\Lambda}^{\mathbf{r}}(\xi)}{d\xi} + G_{21}(x,\xi)S^{\mathrm{l}}(\xi), \quad (59)$$

and the following boundary conditions:

$$G_{21}(x,x)\mathbf{\Lambda}^{\mathbf{r}}(x) + \mathbf{\Lambda}^{\mathbf{l}}(x)G_{21}(x,x) = -S^{\mathrm{o}}(x), \quad (60)$$

$$G_{22}(x,x)\mathbf{\Lambda}^{\mathbf{l}}(x) - \mathbf{\Lambda}^{\mathbf{l}}(x)G_{22}(x,x) = 0, \quad (61)$$

$$G_{21}(x,0)\mathbf{\Lambda}^{\mathbf{r}}(0)Q_0 - G_{22}(x,0)\mathbf{\Lambda}^{\mathbf{l}}(0) = -\Delta(x). \quad (62)$$

The existence, uniqueness and regularity of the backstepping transformation (57) could be guaranteed similarly as Hu et al. (2015), by adding some artificial boundary conditions, for which the proof is omitted here, and then the continuity of the kernels guarantees the existence of a unique inverse transformation. We write the inverse transformation as

$$\begin{pmatrix} u(t,x) \\ v(t,x) \end{pmatrix} = \begin{pmatrix} \epsilon(t,x) \\ \beta(t,x) \end{pmatrix} - \int_0^x \begin{pmatrix} 0 & 0 \\ \mathcal{G}(x,\xi) & \mathcal{H}(x,\xi) \end{pmatrix} \begin{pmatrix} \epsilon(t,\xi) \\ \beta(t,\xi) \end{pmatrix} d\xi, \quad (63)$$

then we could derive from (57) and (63) that the kernels $\mathcal{G}(x,\xi), \mathcal{H}(x,\xi)$ need to satisfy

$$0 = G(x,\xi) + \mathcal{G}(x,\xi) - \int_\xi^x \mathcal{H}(x,\eta)G(\eta,\xi)\, d\eta, \quad (64)$$

$$0 = H(x,\xi) + \mathcal{H}(x,\xi) - \int_\xi^x \mathcal{H}(x,\eta)H(\eta,\xi)\, d\eta. \quad (65)$$

In order to solve the system of equations (64)–(65), we use the method of successive approximations, see, (Krstic and Smyshlyaev, 2008, Section 4.4). In the mean time, $\delta_{i,j}(x)$ for $i = \overline{2,\ m}$ $j = \overline{1,\ m-1}$ can be obtained. And the following equations are obtained for $C^{\mathrm{r}}(x,\xi)$, $C^{\mathrm{l}}(x,\xi)$:

$$C^{\mathrm{r}}(x,\xi) = S^{\mathrm{l}}(x)G_{21}(x,\xi) + \int_\xi^x C^{\mathrm{l}}(x,\eta)G_{21}(\xi,\eta)\, d\eta, \quad (66)$$

$$C^{\mathrm{l}}(x,\xi) = S^{\mathrm{l}}(x)G_{22}(x,\xi) + \int_\xi^x C^{\mathrm{l}}(x,\eta)G_{22}(\xi,\eta)\, d\eta. \quad (67)$$

Hence, the control law $\mathfrak{U}(t)$ can be obtained by substituting transformation (57) into (49). Readily, $\beta(t,1) = 0$ implies that

$$\mathfrak{U}(t) = -R_1 u(t,1) + \int_0^1 [G_{21}(1,\xi)u(t,\xi) + G_{22}(1,\xi)v(t,\xi)]d\xi. \quad (68)$$

3.4 Stability of the Target system

Assume that there exist constants $M > 0, \bar{q} > 0$, such that

$$\|C^r(x,\xi)\|, \|C^l(x,\xi)\|, \|S^{\mathrm{r}}(x)\|, \|S^{\mathrm{l}}(x)\| \le M, \quad \forall x \in [0,1], \xi \in [0,x], \quad (69)$$

$$\|Q_0^T Q_0\| < \bar{q}, \quad (70)$$

where $\|\cdot\|$ denotes the 2-norm, and denote

$$\min\left\{\lambda_i^r(x), \lambda_j^l(x) \mid x \in [0,1], i = \overline{1,n},\ j = \overline{1,m}\right\} = \underline{\lambda}, \quad (71)$$

$$\max\left\{\lambda_i^r(x), \lambda_j^l(x) \mid x \in [0,1], i = \overline{1,n},\ j = \overline{1,m}\right\} = \overline{\lambda}. \quad (72)$$

We first prove exponential stability of the target system (53)-(55). The novelty of the proposed approach compared to Hu et al. (2015), lies in the newly proposed Lyapunov function that needs to be successively determined.

Lemma *1.* For any given initial data $((\epsilon^0)^T,\ (\beta^0)^T)^T = (\epsilon^T(0,\cdot),\ \beta^T(0,\cdot))^T \in \left(\mathcal{L}^2([0,1])\right)^{n+m}$ and under the assumption that C^{r}, $C^{\mathrm{l}} \in \mathcal{C}(\mathbb{T})$, the equilibrium $(\epsilon^T,\ \beta^T)^T = (0,\ 0,\ 0,\ 0)^T$ of the target system (53)-(56) is exponentially stable in the $\mathcal{L}^2$-norm:

$$\|(\epsilon^T(t,\cdot), \beta^T(t,\cdot))^T\|^2_{\mathcal{L}^2} := \int_0^1 \epsilon^T(t,x)\epsilon(t,x) + \beta^T(t,x)\beta(t,x)dx. \quad (73)$$

Proof.
We consider the following Lyapunov function:

$$V(t) = \frac{1}{2}\int_0^1 e^{-\nu x}\epsilon^T(t,x)\mathbf{\Lambda}^{\mathbf{r}}_{\mathbf{inv}}(x)\epsilon(t,x)dx + \frac{1}{2}\int_0^1 (1+x)\beta^T(t,x)D\mathbf{\Lambda}^{\mathbf{l}}_{\mathbf{inv}}(x)\beta(t,x)dx, \quad (74)$$

where $D = \text{diag}\,[d_1\,,\, d_2\,,\,\cdots\,,\, d_{m-1}\,,\, d_m]$, and

$$\mathbf{\Lambda}^{\mathrm{r}}_{\mathrm{inv}}(x) = \text{diag}\left\{\frac{1}{\lambda^{\mathrm{r}}_1(x)},\ldots,\frac{1}{\lambda^{\mathrm{r}}_n(x)}\right\},$$
$$\mathbf{\Lambda}^{\mathrm{l}}_{\mathrm{inv}}(x) = \text{diag}\left\{\frac{1}{\lambda^{\mathrm{l}}_1(x)},\ldots,\frac{1}{\lambda^{\mathrm{l}}_m(x)}\right\}$$

with $(\lambda^{\mathrm{r}}_1(x),\ldots,\lambda^{\mathrm{r}}_n(x)) > 0$, $\left(\lambda^{\mathrm{l}}_1(x),\ldots,\lambda^{\mathrm{r}}_m(x)\right) > 0$. The constants ν and $d_1,\, d_2\,,\,\cdots\,,\, d_{m-1},\, d_m$ are all positive parameters to be determined. Then, we could find two postitive constants C_1, C_2 such that

$$C_1\|(\epsilon(t,\cdot),\beta(t,\cdot))\|^2_{\mathcal{L}^2} \leq V(t) \leq C_2\|(\epsilon(t,\cdot),\beta(t,\cdot))\|^2_{\mathcal{L}^2}, \quad (75)$$

which ensures that $V(t)$ is positive definite.

Differentiating (74) with respect to time, we get:

$$\dot{V}(t) = \int_0^1 e^{-\nu x}\epsilon^T(t,x)\mathbf{\Lambda}^{\mathbf{r}}_{\mathbf{inv}}(x)\partial_t\epsilon(t,x)dx + \int_0^1 (1+x)\beta^T(t,x)D\mathbf{\Lambda}^{\mathbf{l}}_{\mathbf{inv}}(x)\partial_t\beta(t,x)dx. \quad (76)$$

With the help of (53) and (54), we could derive from (76) that

$$\begin{aligned}\dot{V}(t) \leq{}& \beta_1(t,0)^2 \times\left\{\frac{\bar{q}}{2} - \frac{1}{2}d_1 + \int_0^1 \frac{(1+x)}{2}\sum_{i=2}^m d_i^2\frac{1}{\lambda^{\mathrm{l}}_i(x)^2}\delta^2_{i,1}(x)dx\right\}\\
&+ \beta_2(t,0)^2\left\{\frac{\bar{q}}{2} - \frac{1}{2}d_2 + \int_0^1 \frac{(1+x)}{2}\sum_{i=3}^m d_i^2\frac{1}{\lambda^{\mathrm{l}}_i(x)^2}\delta^2_{i,2}(x)dx\right\}\\
&+ \cdots + \beta_{m-1}(t,0)^2\left\{\frac{\bar{q}}{2} - \frac{1}{2}d_{m-1} + \int_0^1 \frac{(1+x)}{2}d_m^2\frac{1}{\lambda^{\mathrm{l}}_m(x)^2}\delta^2_{m,m-1}(x)dx\right\}\\
&+ \beta_m^2(t,0)\left\{\frac{\bar{q}}{2} - \frac{1}{2}d_m\right\}\\
&- \frac{1}{2}f_1(\nu)\int_0^1 e^{-\nu x}\epsilon^T(t,x)\epsilon(t,x)dx\\
&- \frac{1}{2}f_2(\nu)\int_0^1 \beta^T(t,x)\beta(t,x)\,dx \end{aligned} \quad (77)$$

with

$$f_1(\nu) = \nu - 2\left(\frac{M}{\underline{\lambda}}\right)^2 - \frac{M}{\underline{\lambda}}(5+\frac{1}{\nu}), \quad (78)$$

$$f_2(\nu) = \min\left\{d_i; i = \overline{1,m}\right\} - 2m + 1 - \frac{1}{\nu}. \quad (79)$$

First, choose the positive constants $d_1,\, d_2\,,\,\cdots\,,\, d_{m-1},\, d_m$ successively as follows:

$$\begin{aligned} d_m &\geq \bar{q},\\
d_{m-1} &\geq \bar{q} + \int_0^1 (1+x)d_m^2\frac{1}{\lambda^{\mathrm{l}}_m(x)^2}\delta^2_{m,m-1}(x)dx,\\
d_{m-2} &\geq \bar{q} + \int_0^1 (1+x)\sum_{i=m-1}^m d_i^2\frac{1}{\lambda^{\mathrm{l}}_i(x)^2}\delta^2_{i,m-2}(x)dx,\\
&\cdots\\
d_1 &\geq \bar{q} + \int_0^1 (1+x)\sum_{i=2}^m d_i^2\frac{1}{\lambda^{\mathrm{l}}_i(x)^2}\delta^2_{i,1}(x)\,dx. \end{aligned} \quad (80)$$

Then, choose $\nu > 0$ large enough to satisfy

$$f_1(\nu) > 0, f_3(\nu) := \bar{q} - 2m + 1 - \frac{1}{\nu} > 0. \quad (81)$$

from which we have

$$f_2(\nu) \geq f_3(\nu) > 0. \quad (82)$$

Thus, there exists a positive constant c such that

$$\dot{V}(t) \leq J_2(t) \leq -cV(t). \quad (83)$$

This, together with (75), completes the proof.

3.5 *Stability of the closed-loop control system*

With the exponential stability of the target system, and the existence, uniqueness and regularity and invertibility of the backstepping transformation, we are now ready to derive the stability of the closed-loop control system.

Theorem 1. For any given initial data $((u^0)^T,\ (v^0)^T)^T = (u^T(0,\cdot),\ v^T(0,\cdot))^T \in \left(\mathcal{L}^2([0,1])\right)^{n+m}$ and under the assumption that $C^{\mathrm{r}},\ C^{\mathrm{l}} \in \mathcal{C}(\mathbb{T})$, the equilibrium $(u^T,\ v^T)^T = (0,\ 0,\ 0,\ 0)^T$ of the closed-loop system (38)–(50) with the designed controller (68) is exponentially stable in the sense of $\mathcal{L}^2$-norm:

$$\|(u^T(t,\cdot),v^T(t,\cdot))^T\|^2_{\mathcal{L}^2} := \int_0^1 u^T(t,x)u(t,x) + v^T(t,x)v(t,x)dx. \quad (84)$$

Theorem 1 can immediately be applied to the linearized bilayer Saint-Venant model (1), in Riemann Invariants.

4. SIMULATION RESULTS

The goal of the following numerical simulations is to illustrate the efficiency of the designed $\mathfrak{U}(t)$, namely (68), to stabilize the linear system (30) around the zero equilibrium. As initial conditions, the following data are considered for the layer 1 and 2 through the physical variables

$H_2(0,x) = 2 + 0.5\exp\left(-\frac{(x-0.5)^2}{0.003}\right)$, $H_1(0,x) = 6 - H_2(x)$ and

$$U_1(0,x) = \frac{10}{H_1(0,x)} + 3\sin(2\pi x),$$
$$U_2(0,x) = -\frac{10}{H_2(0,x)} - 3\sin(2\pi x).$$

The initial data of the characteristic variables ξ_k, $(k = 1,\,2,\,3,\,4)$ (for system (30)) are computed as function of the physical variables $H_i(0,x)$ and $U_i(0,x)$ for $i = 1,\,2$, thanks to the relation (17). For the sake of simplicity, we consider this uniform steady state: $H_1^* = 3$, $U_1^* =$

1, $H_2^* = 1$, $U_2^* = 0.95$. With this choice of steady state (setpoint), the characteristic speeds are given by: $\lambda_1 = 6.42$, $\lambda_2 = 4.08$, $\lambda_3 = -4.42$ and $\lambda_4 = -2.18$. Elsewhere, in the reported numerical experiments, the ratio r between the densities is set to 0.01 and the friction coefficient C_f to 0.05. We compute the solution up to time $T = 10$. Regarding to the boundary conditions (50) the following matrix are considered

$$Q_0 = \begin{bmatrix} -1.5 & 0.01 \\ 0.01 & 1.5 \end{bmatrix}, \quad R_1 = \begin{bmatrix} 0.5 & 0.1 \\ 0.15 & -0.5 \end{bmatrix} \tag{85}$$

Our implementation is based on an accurate finite volume method for the evolution equation (30), see, a modified Roe's scheme (see LeVeque (2002)). The kernels G_{21} and G_{22} are solved numerically according to (58)-(62) using the finite element setup under the package *FreeFem++* (Hecht (2012)). As an illustration, the numerical solution of the second component of the kernel G_{21} is given in Figure 2.

Figure 3(b) depicts the evolution in time of the $\mathcal{L}^2$-norm of the characteristics. As expected from the theoretical part we observe clearly that the norm of all characteristics decreases in time and converges to zero. As a result, this shows that the system (30) converges to the zero equilibrium. Thereby the two-layer Saint-Venant model (1) also converges to $(H_1^*, U_1^*, H_2^*, U_2^*)$.

In Figure 3(a) are depicted the behavior in time of each component of the input control $\mathfrak{U}(t)$. Clearly, despite the initial amplitude of $\mathfrak{u}_2(t)$, this latter one decreases in time and vanishes after $t \geq 7\,s$. Likewise $\mathfrak{u}_2(t)$, the first component of the control input $\mathfrak{u}_1(t)$ shows the same trend with its amplitude decreasing in time and tending to zero after $t \geq 7s$ as can be seen in Figure 3(a).

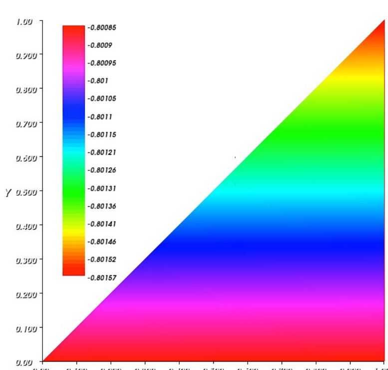

Figure 2. The second component of the kernel G_{21}.

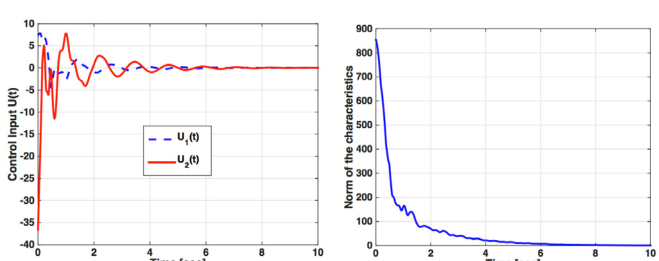

(a) control input (b) Characteristic solutions

Figure 3. Evolution in time of the control input $U(t)$ and the norm of the characteristic solutions

REFERENCES

Abgrall, R. and Karni, S. (2009). Two-layer shallow water system: a relaxation approach. *SIAM J. Sci. Comput.*, 31, No 3, 1603–1627.

Audusse, E., Bristeau, M.O., Perthame, B., and Sainte-Marie, J. (2011). A multilayer saint-venant system with mass exchanges for shallow water flows. derivation and numerical validation. *ESAIM: Mathematical Modelling and Numerical Analysis*, 45(1), 169–200.

Bouchut, F. and Morales, d.L.T. (2008). An entropy satisfying scheme for two-layer shallow water equations with uncoupled treatment. *ESAIM: Mathematical Modelling and Numerical Analysis*, 42, 683–698.

Di Meglio, F., Vazquez, R., and Krstic, M. (2013). Stabilization of a system of coupled first-order hyperbolic linear PDEs with a single boundary input. *IEEE Transactions on Automatic Control*, 58(12), 3097–3111.

Diagne, A., Diagne, M., Tang, S., and Krstic, M. (2016). Backstepping stabilization of the linearized *Saint-Venant-Exner* model. *Automatica, provisionally accepted*.

Hecht, F. (2012). New development in freefem++. *J. Numer. Math.*, 20(3-4), 251–265.

Hu, L., Meglio, F.D., Vazquez, R., and Krstic, M. (2015). Control of homodirectional and general heterodirectional linear cou- pled hyperbolic pdes. *arXiv preprint arXiv:1504.07491*.

Kim, J. and LeVeque, R.J. (2008). Two-layer shallow water system and its applications. In *Proceedings of the Twelth International Conference on Hyperbolic Problems, Maryland*.

Krstic, M. and Smyshlyaev, A. (2008). *Boundary control of PDEs: A course on backstepping designs*, volume 16. Siam.

LeVeque, R.J. (2002). *Finite volume methods for hyperbolic problems*. Cambridge texts in applied mathematics. Cambridge University Press, Cambridge, New York. URL `http://opac.inria.fr/record=b1100566`. Autres tirages : 2003, 2005, 2006.

Majd, M.S. and Sanders, B.F. (2014). The lhllc scheme for two-layer and two-phase transcritical flows over a mobile bed with avalanching, wetting and drying. *Advances in Water Resources*, 67, 16–31.

Munoz-Ruiz, M.L., Chatelon, F.J., and Orenga, P. (2003). On a bi-layer shallow-water problem. *Nonlinear Analysis: Real World Applications*, 4(1), 139–171.

Narbona-Reina, G. and Zabsonre, J.D.D. (2009). Existence of a global weak solution for a 2d viscous bi-layer shallow water model. *Nonlinear Analysis: Real World Applications*, (10), 2971–2984.

Nieto, E.F., Castro-Diaz, M.J., and Parés, C. (July 2011). On an intermediate field capturing riemann solver based on a parabolic viscosity matrix for the two-layer shallow water system. *Journal of Scientific Computing*, Volume 48, Issue 1-3, 117–140.

Savary, C., Bellal, M., and Zech, Y. (2006). Two-layer approach for transcritical flow on mobile bed: nickpoint migration. In *Proc. Int. Conf. River Flow 2006*, 1155–1163.

Schijf, J. and Schonfeld, J. (Sept. (1953)). Theoretical considerations on the motion of salt and fresh water. *Proc. of the Minn. Int. Hydraulics Conv. Joint meeting IAHR and Hyd. Div. ASCE.*, 321–333.